



# $^{40}\text{Ar}/^{39}\text{Ar}$ geochronologic data from samples collected as part of the Southern Nicola Arc Project

Janet E. Gabites and Mitchell G. Mihalynuk



Ministry of  
Mining and  
Critical Minerals

GeoFile 2025-16

**Ministry of Mining and Critical Minerals  
Responsible Mining and Competitiveness Division  
British Columbia Geological Survey**

Recommended citation: Gabites, J.E., and Mihalynuk, M.G., 2025.  $^{40}\text{Ar}/^{39}\text{Ar}$  geochronologic data from samples collected as part of the Southern Nicola Arc Project. British Columbia Ministry of Mining and Critical Minerals, British Columbia Geological Survey GeoFile 2025-16, 9p.

**Front cover:**

Typical topography of the southern Nicola arc viewed to the northwest toward northern Alleyne and southern Crater lakes. Project mapper Martha Henderson is collecting geolocated digital map data. **Photo by Mitch Mihalynuk.**

**Back cover:**

Trachytic hornblende porphyry clast in a conglomerate (Late Triassic) with a similar matrix. Location is adjacent the collection site of sample MMI14-39-15. **Photo by Mitch Mihalynuk.**



Ministry of  
Mining and  
Critical Minerals



# $^{40}\text{Ar}/^{39}\text{Ar}$ geochronologic data from samples collected as part of the Southern Nicola Arc Project

Janet E. Gabites  
Mitchell G. Mihalynuk

Ministry of Mining and Critical Minerals  
British Columbia Geological Survey  
GeoFile 2025-16

# $^{40}\text{Ar}/^{39}\text{Ar}$ geochronologic data from samples collected as part of the Southern Nicola Arc Project



Janet E. Gabites<sup>1\*</sup>, and Mitchell G. Mihalyuk<sup>2a</sup>

<sup>1</sup> Pacific Centre for Isotopic and Geochemical Research, Department of Earth, Ocean and Atmospheric Sciences, University of British Columbia, Vancouver, BC, V6T 1Z4

<sup>2a</sup> British Columbia Geological Survey, Ministry of Mining and Critical Minerals, Victoria, BC, V8W 9N3, Canada

\* retired

<sup>a</sup> Corresponding author: [Mitch.Mihalyuk@gov.bc.ca](mailto:Mitch.Mihalyuk@gov.bc.ca)

Recommended citation: Gabites, J.E., and Mihalyuk, M.G., 2025.  $^{40}\text{Ar}/^{39}\text{Ar}$  geochronologic data from samples collected as part of the Southern Nicola Arc Project. British Columbia Ministry of Mining and Critical Minerals, British Columbia Geological Survey GeoFile 2025-16, 9p.

---

## Abstract

GeoFile 2025-16 contains data that support geochronological studies of the Nicola Group in southern British Columbia. This data release is primarily focused on methodology, quality control data, and results of  $^{40}\text{Ar}/^{39}\text{Ar}$  geochronological analyses of samples collected mainly from the Nicola Group during fieldwork conducted as part of the Southern Nicola Arc Project

**Keywords:**  $^{40}\text{Ar}/^{39}\text{Ar}$  geochronology, thermochronology, Nicola Group, Quesnel terrane, Missezula formation, Iron Mountain formation, Selish formation, Elkhart formation, Shrimpton formation, Copper Mountain suite, Wildhorse suite, Merritt, Princeton, volcanic arc, porphyry copper mineralization

---

## 1. Introduction

GeoFile 2025-16 contains data that support geochronological studies of the Nicola Group in southern British Columbia (Fig. 1). This data release is primarily focused on methodology, quality control data, and results of  $^{40}\text{Ar}/^{39}\text{Ar}$  geochronological analyses of samples collected from the Nicola Group during fieldwork conducted as part of the Southern Nicola Arc Project (SNAP, Mihalyuk and Logan 2013a, b; Mihalyuk et al., 2014a, b, c; Mihalyuk et al., 2015a, b; Friedman et al., 2016; Mihalyuk et al., 2016; Mihalyuk and Diakow, 2020; Fig.2). In a companion paper (Mihalyuk et al., 2025a), data obtained from U-Pb isotopic analyses are presented.

SNAP focussed on systematic quadrangle mapping of ~1000km<sup>2</sup> each year centered on the Summers Creek (2013), and Shrimpton Creek (2014) areas between Princeton and Merritt (Fig. 2; Mihalyuk et al., 2014c; 2015a, b; 2016) and some of the material presented in those reports is paraphrased here for context. Symbolic representations of the data included in this report are presented in the map and figures of Mihalyuk and Diakow (2020) along with stratigraphic data and geochronological data ready for publication at that time. The Mihalyuk and Diakow (2020) release represents the most up-to-date regional geological context for the data presented here; although some fine-tuning of age data is presented in Mihalyuk et al. (2025b) where precise time of deposition (TOD) was determined for key stratigraphic intervals. With these TOD ages, and the data presented here, a four-stage history of Nicola arc growth is further refined: 1) 239-227

Ma, Missezula formation, arc inception and early growth, characterized by bimodal, basalt and rhyolite volcanism; 2) 227-223 Ma, Iron Mountain formation, rapid, voluminous submarine volcanic edifice growth characterized by augite-phyric basalt breccia and flows, which is locally capped by the emergent, lithologically variable Selish formation; 3) 222-210Ma, Elkhart formation, arc extension and denudation, characterized by unconformities, oxidized conglomerate facies and interlayered hornblende-phyric basaltic flows (new TOD at base); 4) 210-201 Ma, Shrimpton formation, arc disruption and contrasting magmatism yielding widespread biotite and apatite-phyric pyroclastics and coeval alkalic, analcime basalt flows (new TOD). Regionally important Copper Mountain suite porphyry copper mineralizing processes continued until late in the latter stage when waning arc magmatism and submergence led to deposition of overlying, increasingly finer-grained sediments and thin tuffaceous layers (new TOD). A province-wide overview of the Late Triassic porphyry copper deposit epoch is presented in Logan and Mihalyuk (2014). Shortly following deposition, Shrimpton formation strata were folded and faulted by thrusts. These structures are inferred to have been cut by Early Jurassic Wildhorse suite plutons (Parrish and Monger, 1989; Breitsprecher and Mortensen, 2004), which also host porphyry-style mineralization (e.g. Brenda deposit, 194-195 Ma; Logan et al., 2011).

In the data release ([BCGS\\_GF2025-16.zip](#)) are Excel files with  $^{40}\text{Ar}/^{39}\text{Ar}$  step heating data and plots for 13 samples: Appendix 1 (JLO13-3-7 hb.xls); Appendix 2 (JLO13-7-9

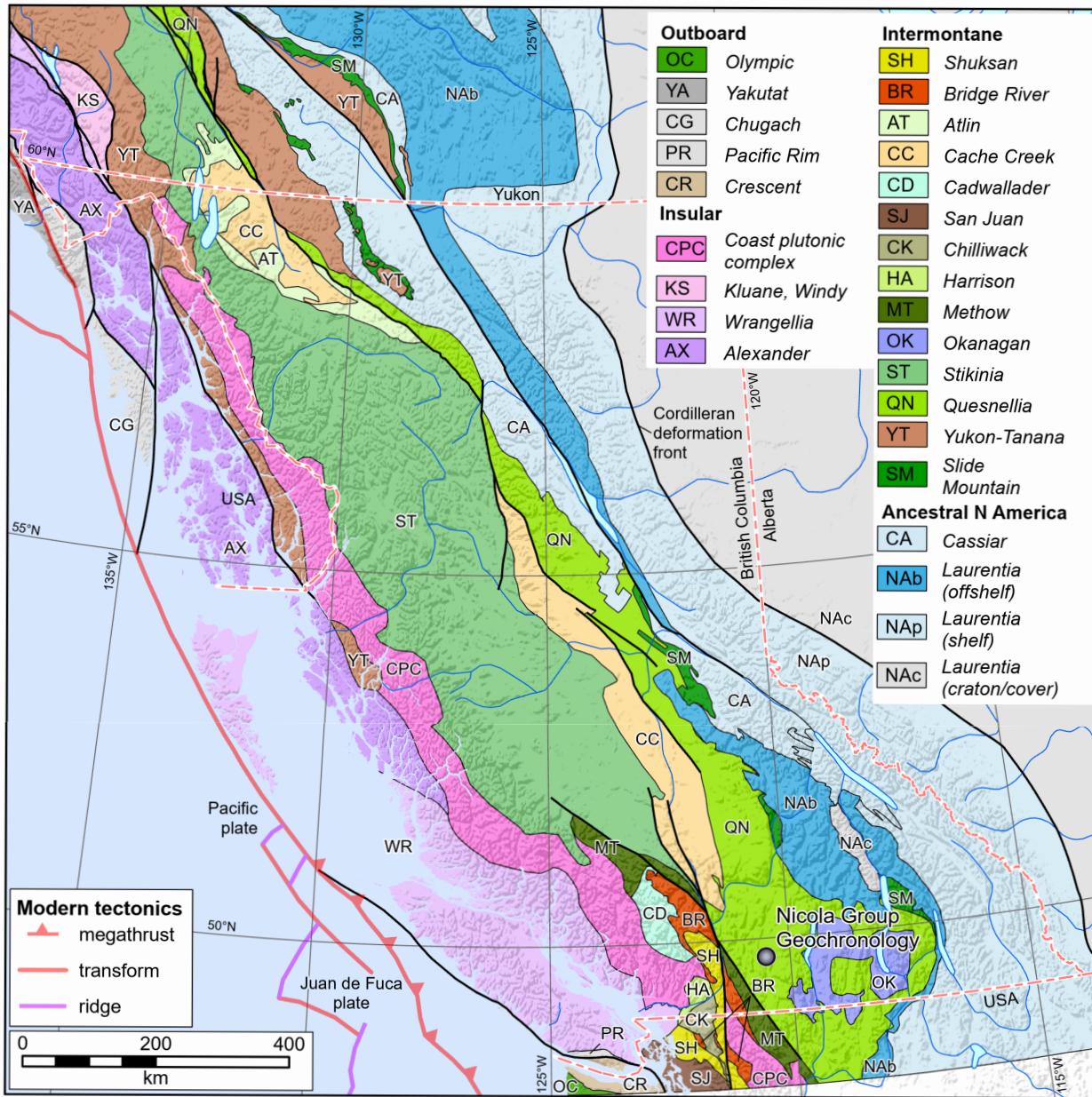


**Fig. 1.** Location, within the Quesnel terrane of southern British Columbia, of the Southern Nicola Arc Project and samples from which the geochronology data reported here were obtained. Terrane map adapted from Wheeler et al., (1991), Colpron and Nelson (2011), and Zagorevski et al. (2021).

hb.xls); Appendix 3 (JLO13-8-4 hb.xls); Appendix 4 (JLO13-23-8-2 bi.xls, JLO13-23-8-2 gm.xls, JLO13-23-8-2 hb.xls); Appendix 5 (LDI14-8-3 (ID906) Hornblende.xls); Appendix 6 (LDI16-1-1b (ID907) Hornblende.xls); Appendix 7 (MMI12-2-8-2 hb.xls); Appendix 8 (MMI12-5-3 bi); Appendix 9 (MMI12-5-8 hb.xls); Appendix 10 (MMI12-8-6 hb.xls) Appendix 11 (MMI13-17-15 gm.xls, MMI13-17-15 hb.xls); Appendix 12 (MMI14-39-15 fs.xls, MMI14-39-15 fs\_rerun.xls, MMI14-39-15 hb\_fine.xls, MMI14-39-15 hb\_pheno.xls, MMI14-39-15 hb\_pheno2.xls); and Appendix 13 (MMI14-60-3 bi.xls).

**2. Methods**

Clean and fresh samples for <sup>40</sup>Ar/<sup>39</sup>Ar analysis were crushed

and sieved to 0.2-0.4mm size fraction. Hornblende, biotite, and feldspar grains were hand picked, washed in nitric acid, rinsed in de-ionized water, dried, wrapped in aluminum foil and stacked in an irradiation capsule with similar-aged samples and neutron flux monitors (Fish Canyon tuff sanidine, 28.175±0.012 Ma (Phillips et al., 2022)). The samples were irradiated at the McMaster Nuclear Reactor in Hamilton, Ontario, for 90 MWh, in a neutron flux of approximately 3 x 10<sup>16</sup> neutrons/cm<sup>2</sup>/s. Samples were analyzed in the Noble Gas Laboratory at the Pacific Centre for Isotopic and Geochemical Research, The University of British Columbia, Vancouver. Each aliquot of mineral separate was step heated at incrementally higher powers until fused using the defocused

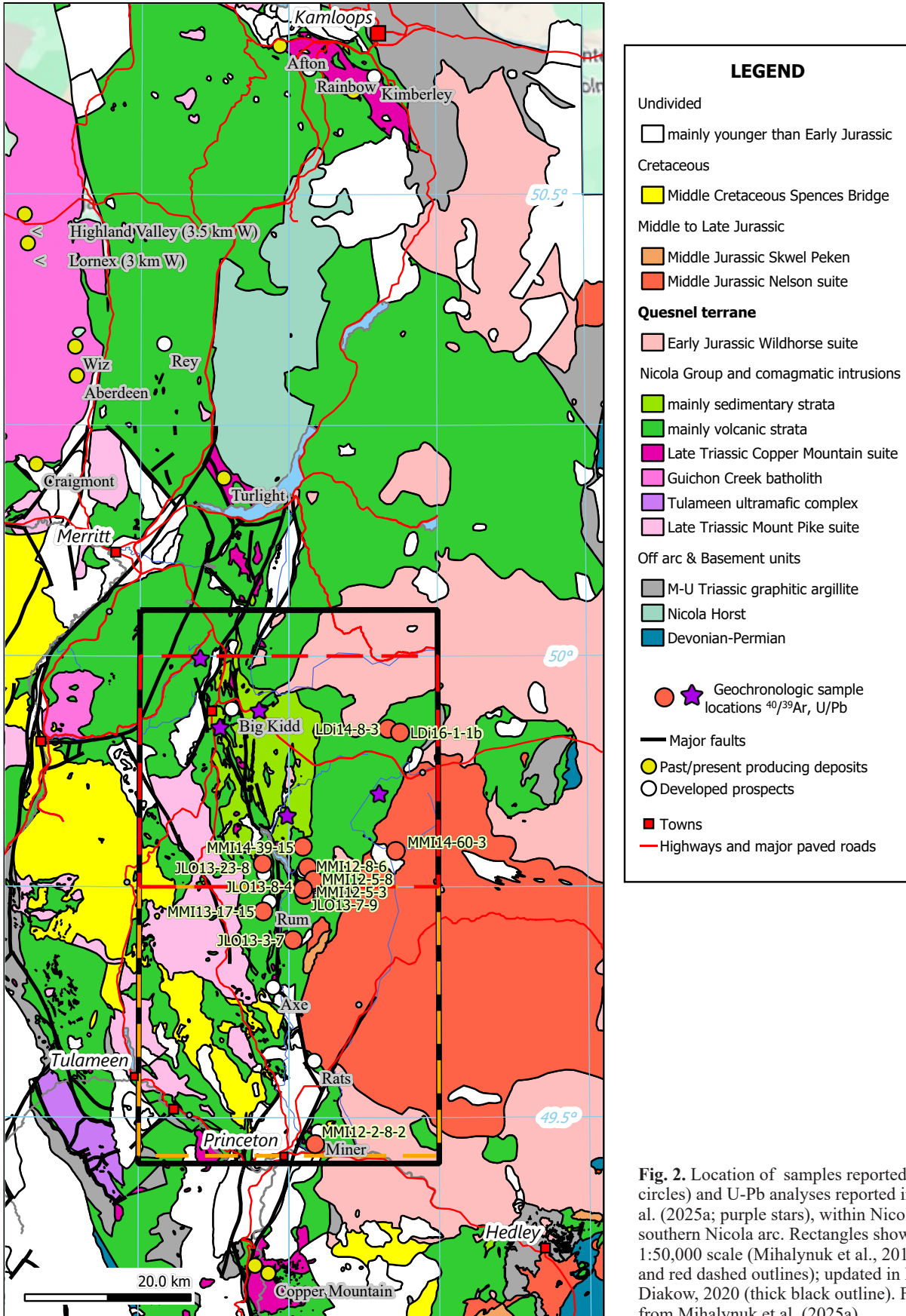


Fig. 2. Location of samples reported here (orange circles) and U-Pb analyses reported in Mihalynuk et al. (2025a; purple stars), within Nicola Group strata of southern Nicola arc. Rectangles show areas mapped at 1:50,000 scale (Mihalynuk et al., 2014c, 2015 (orange and red dashed outlines); updated in Mihalynuk and Diakow, 2020 (thick black outline). Figure adapted from Mihalynuk et al. (2025a).

beam of a 10 W CO<sub>2</sub> laser (New Wave Research MIR10). Gas evolved from each step was analyzed by a VG5400 mass spectrometer equipped with an ion-counting electron multiplier. All measurements were corrected for total system blank, mass spectrometer sensitivity, mass discrimination, radioactive decay during and after irradiation. Decay constants are from Min et al. (2000), and air argon composition from Lee et al. (2006). Also accounted for was Ar interference from atmospheric contamination and the irradiation of Ca, Cl and K (isotope production ratios: [<sup>40</sup>Ar/<sup>39</sup>Ar] K=0.0302 ± 0.00006; [<sup>37</sup>Ar/<sup>39</sup>Ar] Ca=1416.4 ± 0.5; [<sup>36</sup>Ar/<sup>39</sup>Ar] Ca=0.3952 ± 0.0004, Ca/K=1.83 ± 0.01 [<sup>37</sup>Ar<sub>Ca</sub>/<sup>39</sup>Ar<sub>K</sub>]). Ages of heating steps were calculated using ArArCalc (Koppers, 2002). Release spectrum plateaus and correlation ages were calculated using Isoplot v. 3.00 (Ludwig, 2003). Errors are quoted at the 2σ (95% confidence) level and are propagated from all sources except mass spectrometer sensitivity and age of the flux monitor. The minimum justifiable plateau and plateau age were based on the following criteria: three or more contiguous steps comprising more than 50% of the <sup>39</sup>Ar; the probability of fit of the weighted mean age greater than 5%; the slope of the error-weighted line through the plateau ages equals zero at 5% confidence; the ages of the two outermost steps on a plateau are not significantly different from the weighted-mean plateau age (at 1.8σ, six or more steps only); and the outermost two steps on either side of a plateau must not have nonzero slopes with the same sign (at 1.8σ, nine or more steps only).

Where reported, irradiation was: Can 63 180 mWh (samples MMI12-5-8 hb, MMI12-8-6 hb); Can 64 180 mWh, (sample MMI12-5-3 bi); Can 66 160 mWh (sample JLO13-3-7); Can 69 140 mWh (sample JLO13-7-9); Can 70 150 mWh (samples JLO13-8-4, JLO13-23-8-2, MMI13-17-15); and Can 72 134 mWh (samples MMI14-60-3, MMI13-39-15).

### 3. Results

#### 3.1. Sample JLO13-3-7, hornblende: 271.4 ± 5.3 Ma

A good quality plateau including 99.26% of the <sup>39</sup>Ar released yields an age of 271.4 ± 5.3 Ma, consistent with a plateau defined by 84.4% of released, producing an age of 273.4 ± 3.8 Ma (Fig. 3; Appendix 1).

The sample was taken from a massive conglomerate and minor bedded sandstone unit 2.4 km north of Rampart Lake (-120.49267° E, 49.69275° N). Polymictic clasts, mainly volcanic (Nicola Group source), but locally dominated by medium-grained monzonite and diorite, sparse carbonate, and rare gabbro and pyroxenite considered to record deep arc erosion. At the sample site clasts are monolithologic and feldspar-hornblende-phyric with vitreous hornblende up to 1 cm diameter. Although the outcrop appears as if it could be part of a volcanic breccia unit, the unexpectedly old age argues for derivation from an older part of the arc seen nowhere else.

#### 3.2. Sample JLO13-7-9, hornblende: 171.4 ± 1.1 Ma

This sample is from a basaltic andesite lapilli and breccia tuff with conspicuous prismatic hornblende (5-10 mm) and lesser pyroxene phenocrysts collected from an outcrop 3.3 km south-southeast of the south end of Missezula Lake (-120.47355° E, 49.74138° N). A plateau age of 171.4 ± 1.1 Ma, representing 81.1% of the <sup>39</sup>Ar released (Fig. 4; Appendix 2), is considered to be reset, possibly in the thermal halo of the enormous Osprey

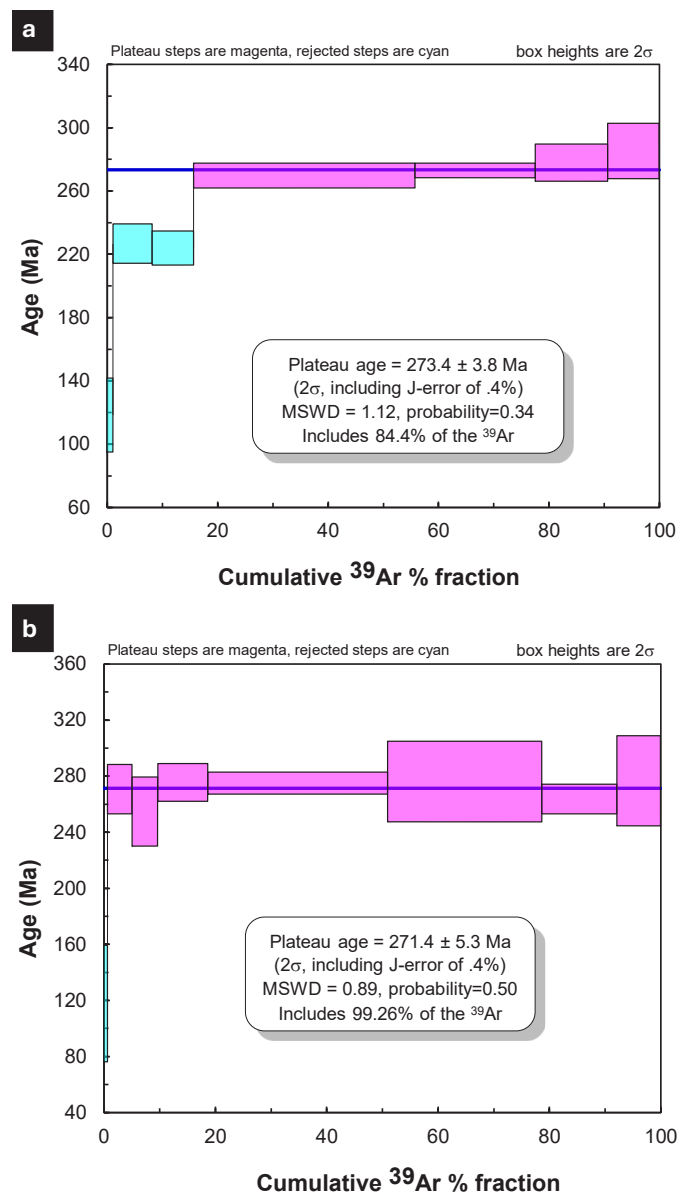


**Fig. 3. a)** Argon release spectrum for hornblende separated from sample JLO13-3-7; **b)** rerun with a good quality 271.4 ± 5.3 Ma plateau including 99.26% of <sup>39</sup>Ar released; see Appendix 1.

Lake granitoid complex (ca.165 Ma; Mihalynuk et al., 2015, 2016) 3.5 km to the southeast.

#### 3.3. Sample JLO13-8-4, hornblende: 183.2 ± 1.6 Ma

A sample of coarse hornblende-phyric basalt was collected ~2.6 km south-southeast of the southern end of Missezula Lake (-120.47646° E, 49.74775° N). A tight plateau age of 183.2 ± 1.6 Ma, representing 63.6% of the <sup>39</sup>Ar released (Appendix 3), is considered reset by the nearby intrusions related to the Pennask complex (ca. 195 crystallization to 183 Ma cooling; Mihalynuk et al., 2015a, 2016) or partially reset in the thermal halo of the enormous Osprey Lake granitoid complex (ca.165 Ma; Mihalynuk et al., 2015a, 2016) 4 km to the southeast.

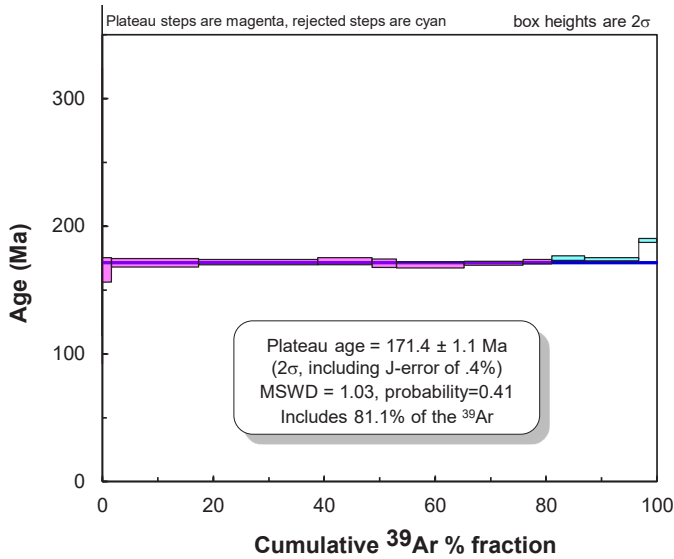


Fig. 4. Argon release spectrum for hornblende separated from sample JLO13-7-9; see Appendix 2.

**3.4. Sample JLO13-23-8-2, secondary biotite: 165.3 ± 4.7 Ma**

A sample of brecciated and biotite-altered hornblende diorite was collected ~1.3 km east of southern Ketchum Lake (-120.47932° E, 49.74439° N). Multiple attempts were made to extract geologically meaningful cooling ages from the sample. The oldest age obtained was a plateau age from secondary biotite of 165.3 ± 4.7 Ma, representing 72.9% of the <sup>39</sup>Ar released (Appendix 4). Release spectra from hornblende phenocrysts and the rock matrix yielded plateau ages of 124.5 ± 2.8 Ma and 116.72 ± 0.71 Ma respectively. Although a Late Jurassic potassic alteration event is suggested (coeval with the Osprey batholith exposed 10 km southeast), a reliable interpretation will require additional information.

**3.5. Sample LDI14-8-3 (ID906), hornblende: 210 ± 1.8 Ma**

This is a sample of Elkhart formation basalt that is dark green,

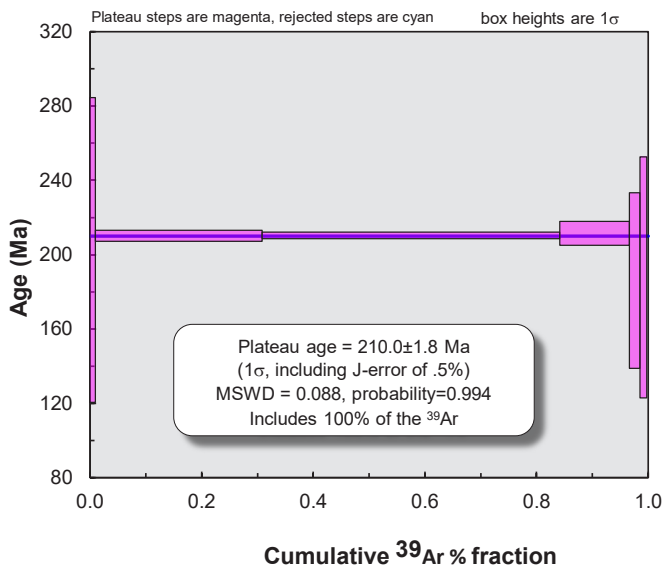


Fig. 5. Argon release spectrum for hornblende separated from sample LDI14-8-3; see Appendix 5.

medium-to coarse-porphyritic and amygdaloidal and containing phenocrysts of plagioclase, pyroxene, and prismatic hornblende. The sample was collected 1.4 km from the south end of Boot Lake (-120.33380° E, 49.92144° N). A high quality plateau defined by 100% of <sup>39</sup>Ar released yields an age of 210.0 ± 1.8 Ma (Fig. 5; Appendix 5,) considered to be the age of basalt extrusion.

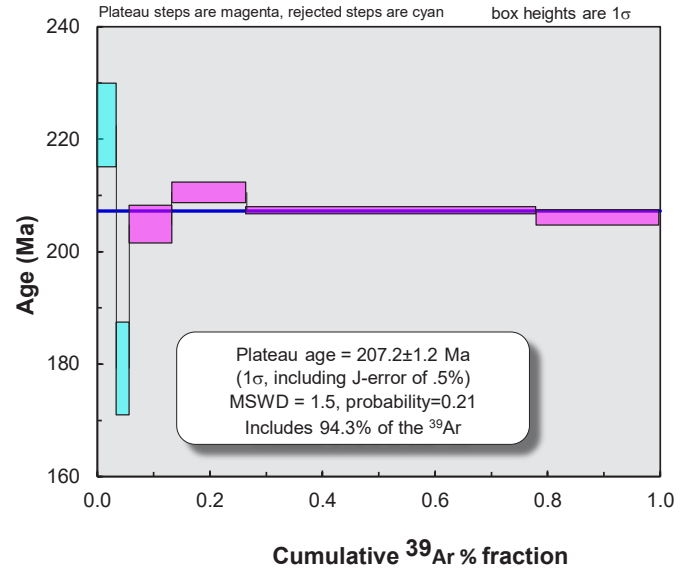


Fig. 6. Argon release spectrum for hornblende separated from sample LDI16-1-1b; see Appendix 6).

**3.6. Sample LDI16-1-1b (ID907), hornblende: 207.2 ± 1.2 Ma**

This sample is from a plagioclase, pyroxene and prismatic hornblende-porphyritic dike cutting polymictic conglomerate of the Elkhart formation. The sample was collected 2.7 km from the south end of Boot Lake (-120.31375° E, 49.91729° N). A high quality plateau defined by 94.3% of Ar released yields an age of 207.2 ± 1.2 Ma (Fig. 6; Appendix 6), interpreted as the age of dike cooling immediately following intrusion.

**3.7. Sample MMI12-2-8-2, hornblende: 183.4 ± 3.5 Ma (disturbed)**

This is a sample of hornblende-phyric breccia from the Elkhart formation collected 1 km from the communications tower at Miner Mountain (-120.4563° E, 49.4713° N). The cooling age (Fig. 7; Appendix 7) probably reflects resetting due to thermal effects of nearby Bromley batholith, about 2 km to the southeast and with major apophyses/dikes that are mapped to within 700 m of the sample site (Mihalyuk et al., 2013a, 2014c).

**3.8. Sample MMI12-5-3; secondary biotite: 166 ± 2 Ma**

Three separate analyses (Appendix 8), all equivalent within uncertainty, yielded plateau ages of 166.0 ± 2.0 Ma (Fig. 8a); 164.1 ± 1.4 Ma (Fig. 8b); and 164.0 ± 1.0 Ma (Fig. 8c). This sample is from an Iron Mountain formation basaltic unit in a screen surrounded by Wildhorse suite (Early Jurassic) tonalite/diorite (hornblende diorite altered to epidote-chlorite-actinolite and very fine-grained biotite). It was collected 3.2 km from the south end of Missezula Lake (-120.45988 E, 49.75505 N). The cooling age was meant to date the timing of alteration/mineralization to determine if it is the same as the magmatic

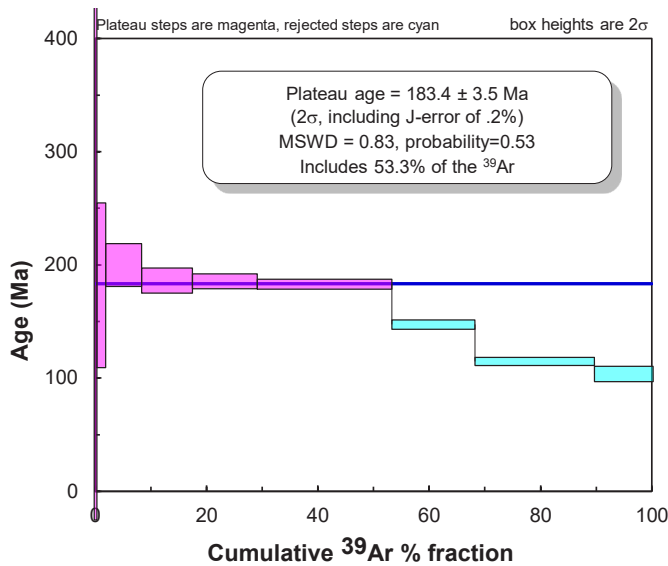


Fig. 7. Argon release spectrum for hornblende separated from sample MMI12-2-8-2; see Appendix 7.

cooling age, and/or alteration in the immediate hangingwall of a thrust cut by Wildhorse intrusions. The Middle Jurassic age is similar to that of the Osprey igneous complex, 5 km to the east (Mihalynuk et al., 2013b, 2015a, 2016).

**3.9. Sample MMI12-5-8; hornblende: 189.0 ± 1.4 Ma**

The sample was collected 3.1 km from the south end of Missezula Lake (-120.45850 E, 49.75775 N) from a dike exposed in intermittent outcrops extending along an east-southeast trend for about 1km and interpreted as part of a single intrusion (Mihalynuk and Diakow, 2020) that cuts older intrusions. A high quality plateau is defined by 100% of the <sup>39</sup>Ar released from the hornblende analyzed and yields an age of 189.0 ± 1.4 Ma (Fig. 9; Appendix 9), interpreted as the intrusive age of the dike.

**3.10. Sample MMI12-8-6; hornblende: 184.4 ± 1.7 Ma (reset)**

A sample of the very coarse hornblende-phyric portion was sampled 2.2, km from the south end of Missezula Lake (-120.46853° E, 49.77129° N) for <sup>40</sup>Ar/<sup>39</sup>Ar dating (Mihalynuk and Logan, 2013a) from a unit of dark green, medium to coarse pyroxene and prismatic hornblende basalt and andesite flow and flow breccia interbedded with minor conglomerate. A good quality plateau is defined by 94.6% of the <sup>39</sup>Ar released and yields an age of 184.4 ± 1.7 Ma (Fig. 10, Appendix 10). Despite the strong plateau, we interpret this to be a reset age, perhaps due to plutons less than 2 km to the west and 4 km to the east (Mihalynuk and Logan, 2013a; Mihalynuk and Diakow, 2020). As demonstrated by sample MMI14-39-15 below, sampling hornblende from the rock body may lead to better success at obtaining a crystallization age, than does analyzing an extract of the very coarse hornblende crystals.

**3.11. Sample MMI13-17-15; hornblende, 187.3 ± 1.3 Ma (disturbed); groundmass 92.7 ± 0.7 Ma (highly disturbed)**

This sample is from a unit of basaltic andesite porphyry with acicular hornblende (vitreous, medium-grained) that defines a trachytic fabric. It was collected 5.7 km from the south end

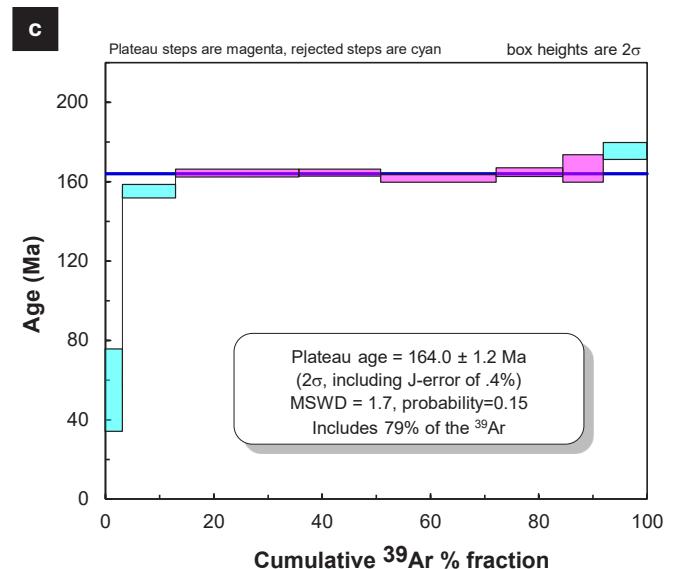
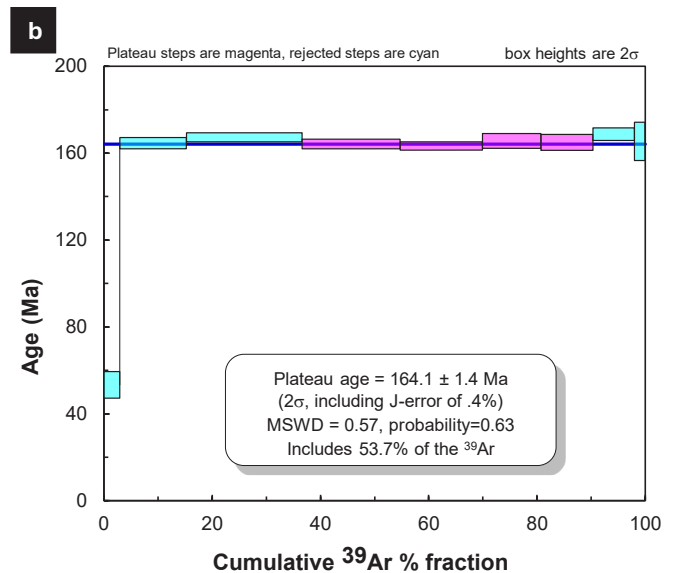
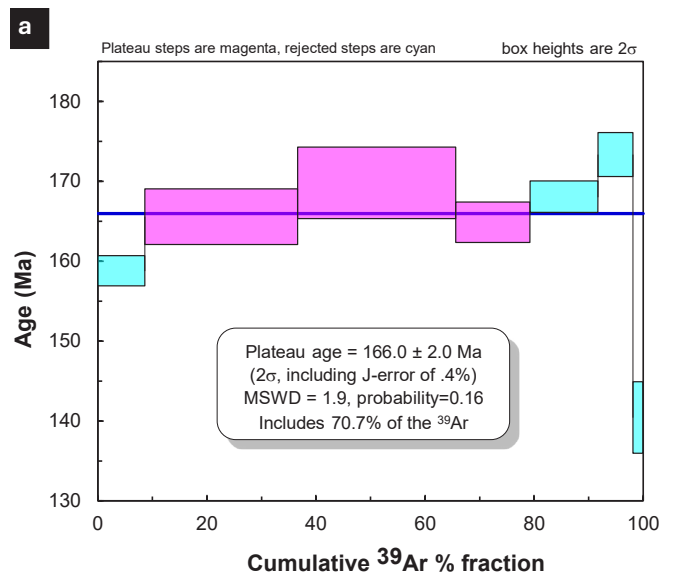


Fig. 8. Argon release spectrum for secondary biotite separated from sample MMI12-5-3 in repeated runs; see Appendix 8.

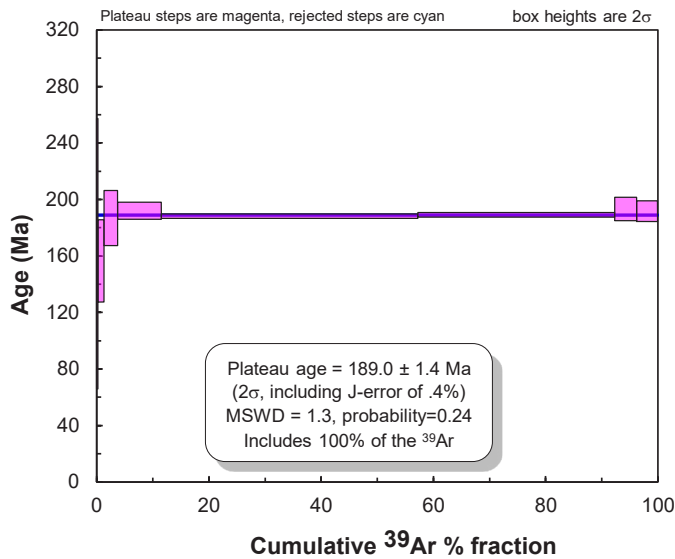


Fig. 9. Argon release spectrum for hornblende separated from sample MMI12-5-8; see Appendix 9.

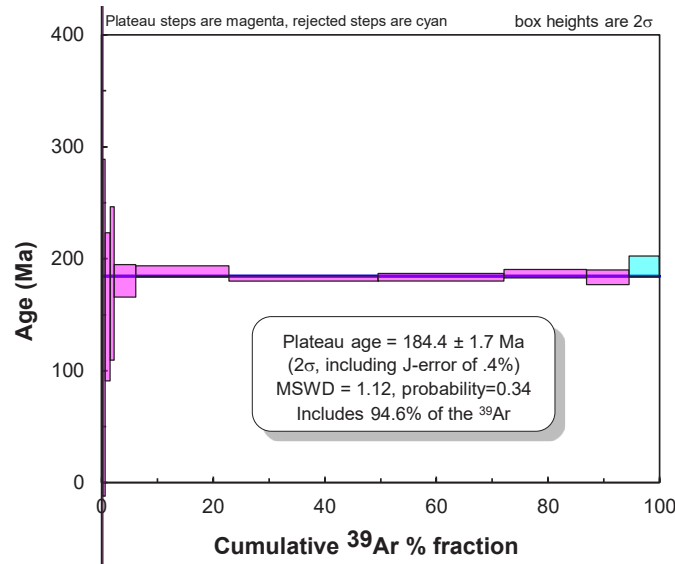


Fig. 10. Argon release spectrum for hornblende separated from sample MMI12-8-6; see Appendix 10.

of Missezula Lake (-120.54110° E, 49.72408° N). A disturbed plateau yields an age of  $187.3 \pm 1.3$  Ma (Fig. 11a, Appendix 11). The hornblende age likely reflects partial resetting, possibly due to heating by the nearby ~1.5 km long quartz diorite stock, the contact of which may be less than 200 m to the east (Mihalynuk and Diakow, 2020). The young groundmass age (Fig. 11b) is geologically meaningless, reflecting continued argon loss.

**3.12. Sample MMI14-39-15, hornblende: 204.6 ± 1.8 Ma (best age)**

This sample was collected from a clast of hornblende porphyry that is the predominant clast type in a conglomerate adjacent a thrust fault 3.2 km northeast of the south end of Missezula Lake (-120.47671° E, 49.79367° N). The aim was to determine if the release spectrum could reveal the age of

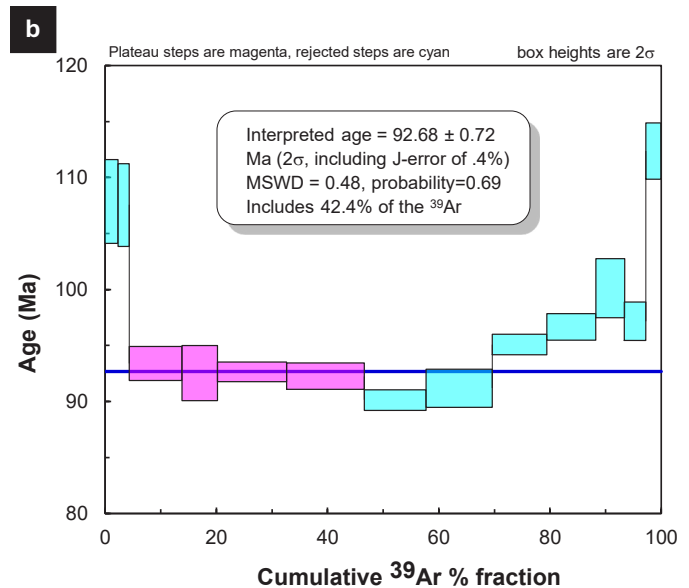
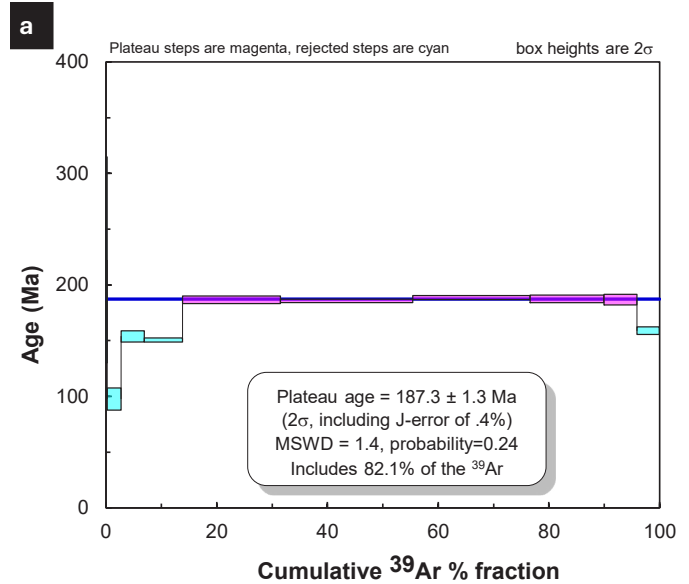


Fig. 11. Argon release spectrum for sample MMI13-17-15 for a) hornblende, b) groundmass; see Appendix 11.

hydrothermal alteration along the thrust and thereby further constrain the age of deformation. A good quality plateau defined by 93.5% of the  $^{39}\text{Ar}$  released yields an age of  $204.6 \pm 1.8$  Ma (Fig. 12a; Appendix 12) and is interpreted to represent the crystallization age of medium-grained hornblende within the unit. However, phenocryst hornblende (Fig. 12 b, c) and feldspar (Fig. 12 d, e) are less Ar-retentive, and their release spectra reflect resetting, possibly on account of emplacement of the huge Osprey igneous complex 7km to the east (Mihalynuk and Diakow, 2020).

**3.13. Sample MMI14-60-3, biotite: 55.5 ± 0.9 Ma**

This sample, collected on the west side of the Galena logging road, 1km from the confluence of Galena and Siwash creeks (-120.32129° E, 49.78894° N), is of a biotite-phyric

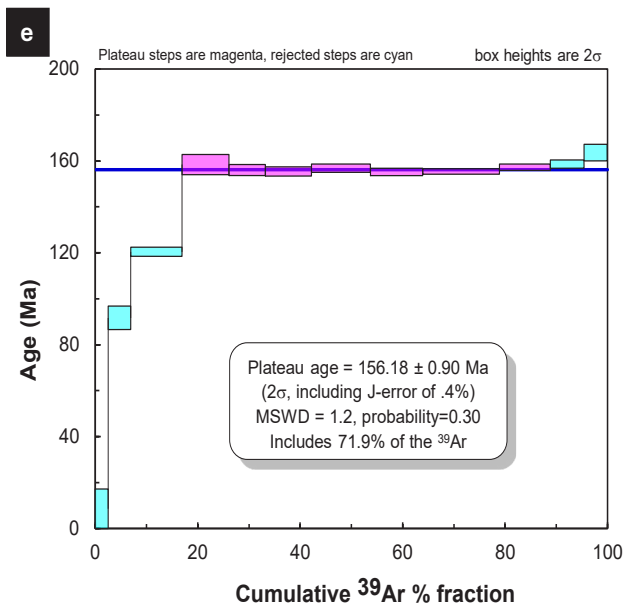
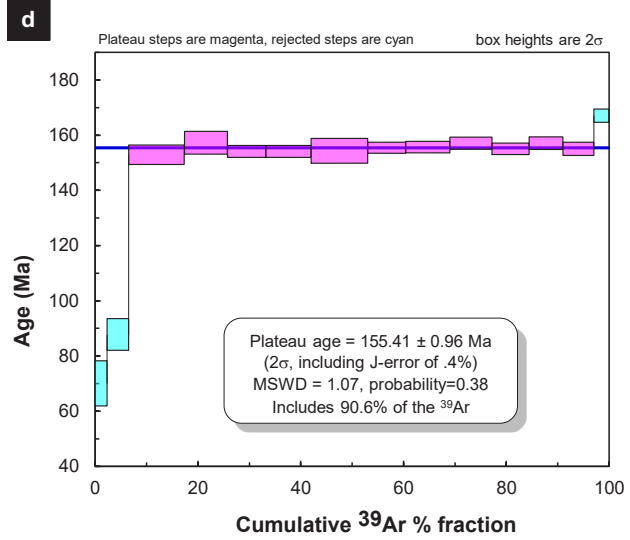
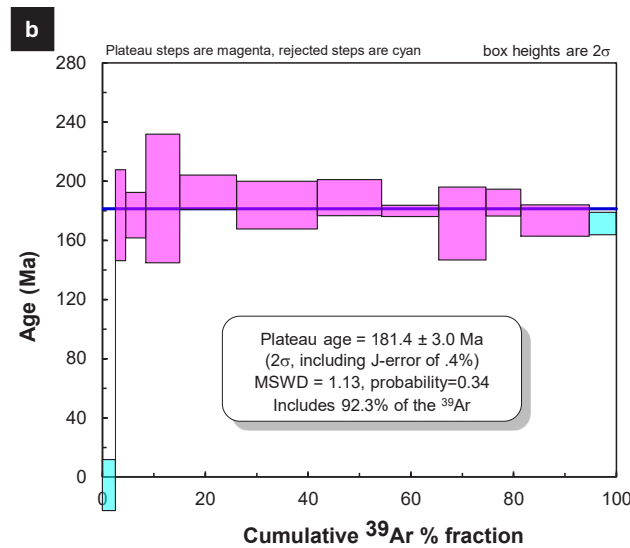
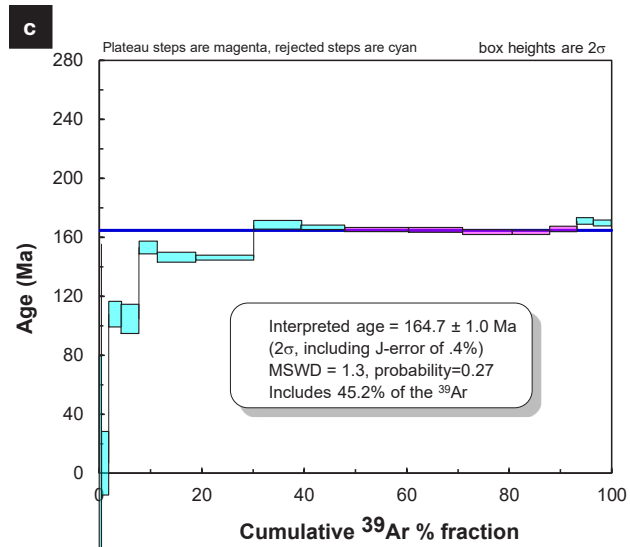
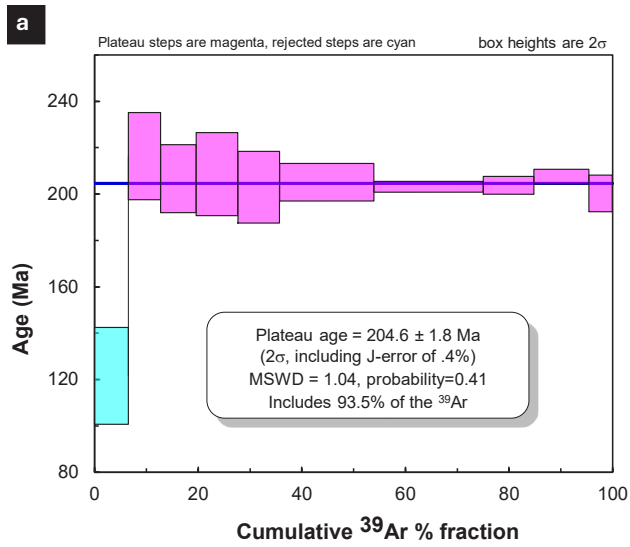


Fig. 12. Argon release spectra for sample MMI14-39-15; a) hornblende; b) and c) hornblende phenocryst; d) feldspar; e) feldspar rerun; see Appendix 12.

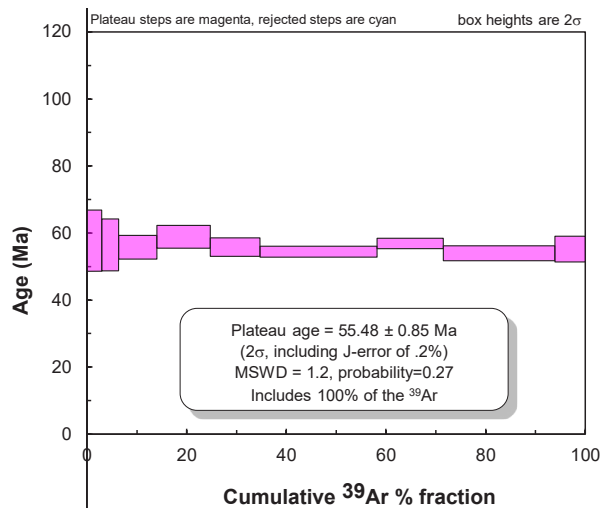


Fig. 13. Argon release spectrum for biotite separated from sample MMI14-60-3; see Appendix 13.

felsic tuff. A plateau including 100% of the  $^{39}\text{Ar}$  released yields an age of  $55.5 \pm 0.9$  Ma and confirms correlation with volcanic rocks of from the Princeton Group, interpreted as comagmatic with hypabyssal intrusive rocks at the nearby Snowstorm prospect (53.4 Ma; U-Pb, cf. Mihalynuk et al., 2015a, 2016).

### Acknowledgment

Larry Diakow (retired) and James Logan (retired) collected some of the samples (numbers prefixed with LDI and JLO) that we report on here.

### References cited

Breitsprecher, K., and Mortensen, J.K., 2004. BCAGE 2004A-1-a database of isotopic age determinations for rock units from British Columbia. British Columbia Ministry of Energy and Mines, British Columbia Geological Survey Open File, v. 3.

Colpron, M., and Nelson, J.L., 2011. A digital atlas of terranes for the northern Cordillera. British Columbia Ministry of Energy and Mines, British Columbia Geological Survey GeoFile 2011-11.

Friedman, R.M., Mihalynuk, M.G., Diakow, L.J., and Gabites, J.E., 2016. Southern Nicola Arc Project 2015: Geochronologic data constraining Nicola Arc history along a transect near  $50^\circ\text{N}$ . British Columbia Ministry of Energy and Mines, British Columbia Geological Survey GeoFile 2016-3, 19p.

Koppers, A.A.P., 2002. ArArCALC – software for  $^{40}\text{Ar}/^{39}\text{Ar}$  age calculations. *Computers and Geosciences*, 28, 605-619.

Lee, J.-Y., Marti, K., Severinghaus, J.P., Kawamura, K., Yoo, H.-S., Lee, J.B., and Kim, J.S., 2006. A redetermination of the isotopic abundances of atmospheric Ar. *Geochimica et Cosmochimica Acta*, 70, 4507-4512.

Logan, J.M., and Mihalynuk, M.G., 2014. Tectonic controls on Early Mesozoic paired alkaline porphyry deposit belts (Cu-Au  $\pm$  Ag-Pt-Pd-Mo) within the Canadian Cordillera. *Economic Geology*, 109, 827-858.

Logan, J.M., Mihalynuk, M.G., Friedman, R.M., and Creaser, R.A., 2011. Age constraints of mineralization at the Brenda and Woodjam Cu-Mo $\pm$ -Au porphyry deposits - An Early Jurassic calcalkaline event, south-central British Columbia. In: *Geological Fieldwork 2010*, British Columbia Ministry of Forests, Mines and Lands, British Columbia Geological Survey Paper 2011-01, pp. 129-144.

Ludwig, K.R., 2003. *Isoplot 3.09 A Geochronological toolkit for Microsoft Excel*. Berkeley Geochronology Center, Special Publication No. 4

Mihalynuk, M.G., and Diakow, L.J., 2020. Southern Nicola arc geology (NTS 92H/7NE, 8NW, 9W, 10E, 15E, 16W, 92I/1SW, 2SE). British Columbia Ministry of Energy, Mines and Low Carbon Innovation, British Columbia Geological Survey Geoscience Map 2020-01, scale 1:50000, 2 sheets.

Mihalynuk, M.G., and Logan, J.M., 2013a. Geological setting of Late Triassic porphyry Cu-Au mineralization at Miner Mountain, Princeton, southern British Columbia. In: *Geological Fieldwork 2012*, British Columbia Ministry of Energy, Mines, and Natural Gas, British Columbia Geological Survey Paper 2013-1, pp. 81-96.

Mihalynuk, M.G., and Logan, J.M., 2013b. Geological setting of Late Triassic porphyry Cu-Au mineralization at the Dillard Creek property near Merritt, southern British Columbia. In: *Geological Fieldwork 2012*, British Columbia Ministry of Energy, Mines and Natural Gas, British Columbia Geological Survey Paper 2013-1, pp. 97-114.

Mihalynuk, M.G., Logan, J.M., Diakow, L.J., Friedman, R.M., and Gabites, J., 2014a. Southern Nicola Arc Project (SNAP): preliminary results. In: *Geological Fieldwork 2013*, British Columbia Ministry of Energy and Mines, British Columbia Geological Survey Paper 2014-1, pp. 29-57.

Mihalynuk, M.G., Friedman, R.M., Gabites, J.E., and Logan, J.M., 2014b. Southern Nicola Arc Project 2013: Geochronological data. British Columbia Ministry of Energy and Mines, British Columbia Geological Survey GeoFile 2014-3, 7p.

Mihalynuk, M.G., Logan, J.M., Diakow, L.J., Henderson, M.A., Jacob, J., and Watson, A.K.G., 2014c. Summers Creek area preliminary geology, NTS 92H/9W & 10E. British Columbia Ministry of Energy and Mines, British Columbia Geological Survey Open File 2014-5, 1:50,000 scale.

Mihalynuk, M.G., Diakow, L.J., Logan, J.M., and Friedman, R.M., 2015a. Preliminary geology of the Shrimpton Creek area (NTS 092H/15E, 16W) Southern Nicola Arc Project. In: *Geological Fieldwork 2014*, British Columbia Ministry of Energy and Mines, British Columbia Geological Survey Paper 2015-1, pp. 129-163.

Mihalynuk, M.G., Friedman, R.M., and Logan, J.M., 2015b. Southern Nicola Arc Project 2014: Geochronological data. British Columbia Ministry of Energy and Mines, British Columbia Geological Survey Geofile 2015-2, 7p.

Mihalynuk, M.G., Diakow, L.J., Friedman, R.M., and Logan, J.M., 2016. Chronology of southern Nicola arc stratigraphy and deformation. In: *Geological Fieldwork 2015*, British Columbia Ministry of Energy and Mines, British Columbia Geological Survey Paper 2016-1, pp. 31-63.

Mihalynuk, M.G., Friedman, R.M., and Wall, C., 2025a. U-Pb geochronologic data from samples collected as part of the Southern Nicola Arc Project. British Columbia Ministry of Mining and Critical Minerals, British Columbia Geological Survey GeoFile 2025-15, 7p.

Mihalynuk, M.G., Wall, C., and Zagorevski, A., 2025b. Time of deposition refinements for key stratigraphic intervals of the Nicola Group, southern British Columbia. In: *Geological Fieldwork 2024*, British Columbia Ministry of Mining and Critical Minerals, British Columbia Geological Survey Paper 2025-01, pp. 105-118.

Min, K., Mundil, R., Renne, P.R., and Ludwig, K.R., 2000. A test for systematic errors in  $^{40}\text{Ar}/^{39}\text{Ar}$  geochronology through comparison with U/Pb analysis of a 1.1-Ga rhyolite. *Geochimica et Cosmochimica Acta*, 64, 73-98.

Parrish, R.R., and Monger, J.W.H., 1992. New U-Pb dates from southwestern British Columbia: In: *Radiogenic age and isotopic studies Report 5*, Geological Survey of Canada Paper 91-2, pp. 87-108.

Phillips, D., Matchan, E.L., Dalton, H., and Kuiper, K.F., 2022. Revised astronomically calibrated  $^{40}\text{Ar}/^{39}\text{Ar}$  ages for the Fish Canyon Tuff sanidine-closing the interlaboratory gap. *Chemical Geology*, 597, article 120815. <https://doi.org/10.1016/j.chemgeo.2022.120815>

Wheeler, J.O., Brookfield, A.J., Gabrielse, H., Monger, J.W.H., Tipper, H.W., and Woodsworth, G.J., 1991. Terrane map of the Canadian Cordillera, Geological Survey of Canada Map 1713A, 2 sheets, scale 1:2,000,000.

Zagorevski, A., van Staal, C.R., Bédard, J.H., Bogatu, A., Canil, D., Coleman, M., Golding, M., Joyce, N.L., Lawley, C., McGoldrick, S., Mihalynuk, M.G., Milidragovic, D., Parsons, A., and Schiarizza, P., 2021. Overview of Cordilleran oceanic terranes and their significance for the tectonic evolution of the northern Cordillera. In: Ryan, J.J. and Zagorevski, A., (Eds.), *Northern Cordillera geology: a synthesis of research from the Geo-mapping for Energy and Minerals program*, British Columbia and Yukon. Geological Survey of Canada Bulletin 610, pp. 21-65. <https://doi.org/10.4095/326053>



Ministry of  
Mining and  
Critical Minerals

